Report no. changed (Mar 2006): SM-366-UU
SACLANTCEN MEMORANDUM
serial no: SM- 366

SACLANT UNDERSEA RESEARCH CENTRE REPORT

Inverse acoustical determination of photosynthetic oxygen productivity of Posidonia seagrass

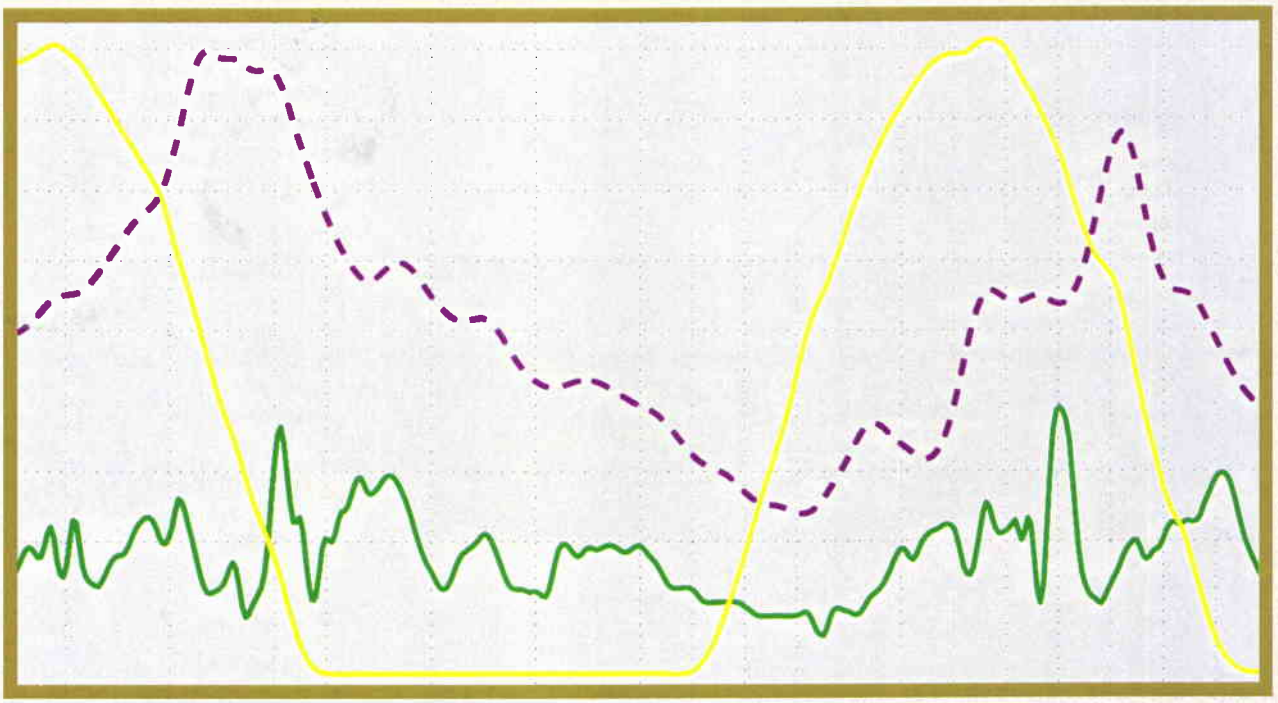

Jean-Pierre Hermand,
Pamela Nascetti and Francesco Cinelli

February 2000

NORTH ATLANTIC TREATY ORGANIZATION ORGANISATION DU TRAITE DE L'ATLANTIQUE NORD

Inverse Acoustical Determination of Photosynthetic Oxygen Productivity of Posidonia Seagrass

J.-P. Hermand, P. Nascetti, F. Cinelli

The content of this document pertains to work performed under Project 01-B of the SACLANTCEN Programme of Work. The document has been approved for release by The Director, SACLANTCEN.

Jan L. Spoelstra
Director

intentionally blank page

Inverse Acoustical Determination of Photosynthetic Oxygen Productivity of Posidonia Seagrass

J.-P. Hermand, P. Nascetti, F. Cinelli

Executive Summary: Mine detection in the shallow waters of the Mediterranean Sea is often limited by the background interference generated from the seabed. The interference is generally in the form of reverberation at mine hunting frequencies from the water-bottom interface. Particular to the Mediterranean Sea are fields of dense Posidonia sea grass. Posidonia affects mine hunting systems by the reverberation produced by the sea grass and oxygen bubbles. The bubbles are generated by photosynthesis and are deposited on the Posidonia leaf blades. Low frequency acoustic inversion techniques, developed to estimate the geoacoustic properties of the seabed, were successfully applied to monitoring the oxygen synthesis of the Posidonia. In this paper there are analyses of the low frequency acoustic data and its correlation with environmental observations of the solar radiation, oxygen, and other factors such as salinity and temperature as a function of depth. The most evident feature is an abrupt and marked change of attenuation and time dispersion characteristics at the onset of photosynthesis. These diurnal phenomena are attributed to bubbles of photosynthetic oxygen formed on the Posidonia leaf blades. It remains to be verified that the effects of Posidonia on higher frequency mine detection systems have a diurnal dependence. The contribution of photosynthetic oxygen to the acoustic attenuation and scattering process requires quantification. In addition to MCM, these results are also relevant to ASW in lottoral waters. Furthermore, these results may be applicable to the monitoring of the state of health of Posidonia and other seagrasses in the Mediterranean and other seas.

intentionally blank page

Inverse Acoustical Determination of Photosynthetic Oxygen Productivity of Posidonia Seagrass

J.-P. Hermand, P. Nascetti, F. Cinelli

Abstract: As part of geoacoustic inversion experiments (Yellow Shark) in the Giglio basin, off the west coast of Italy, low frequency, broad-band propagation measurements were performed in the winter and spring of 1995 over a dense and extensive prairie of Posidonia seagrasses which surrounds Scoglio d'Africa, a minor island of the Tuscan Archipelago. The purpose of the measurements was to determine the applicability of model-based, geoacoustic inversion techniques developed for marine sediments to the monitoring of oxygen synthesis by Posidonia. A dual-flextensional acoustic projector and a 4-element vertical receiving array were positioned at 1541 m distance in an isobath (25 m water depth), dense and homogeneous part of the Posidonia prairie. The waveguide impulse response was measured during one day by 1 min repeated and alternated transmissions of 3 s chirp signals with frequency bands 0.1–0.9 kHz and 0.8–1.6 kHz. The water sound speed profiles calculated from repeated CTD measurements were slightly downward refracting and exhibited little temporal variability except for mild surface heating in the afternoon. Contemporaneous oxygen and CTD profiles as a function of daytime and season were obtained in 1997 to support the present study. In this paper acoustic, solar radiation, oxygen and CTD data are analyzed and discussed. The analysis shows strong correlation between photosynthesis and the impulse response of the acoustic waveguide. The most evident feature is an abrupt and marked change of attenuation and time dispersion characteristics at the onset of photosynthesis. Frequency- and depth-dependent rapid variations of received energy (2–5 dB) and time spread (3–10 ms) are observed. The time of occurence and rate of change of these variations are consistent with solar time and oxygen concentration measured in situ. The phenomena is attributed to bubbles of photosynthetic oxygen formed on the Posidonia leaf blades. The bubble layer creates an absorbing, dispersive, low-speed, thin parallel waveguide which modifies interaction of acoustic energy with the Posidonia "matte". It is demonstrated that, after sunrise, low-order modes begin to travel in the seagrass layer, absorbing a portion of acoustic energy from the main waveguide. A similar effect can occur in a near-surface waveguide when supersaturation (undissolved oxygen) conditions obtain. Modeling results indicate that the inverse problem of determining gas and oxygen void fractions in the seagrass layer could be solved. Parameters such as surface density and photosynthetic efficiency of Posidonia can be derived from the variations of inverted void fractions. These results may be applicable to the monitoring of the state of health of Posidonia and other seagrasses in the Mediterranean and other oceans.

Contents

1 Introduction 1

2 Yellow Shark Posidonia Experiments 2
2.1 Acoustic Measurements Configuration 2
2.2 Broad-Band Acoustic Transmissions 2
2.3 Hydrographic and Irradiance/Oxygen Measurements 4
2.4 Posidonia Plants and Substratum 8
2.5 Time-Varying Waveguide Impulse Response 8

3 Oxygen Measurements in Posidonia Waters 10
3.1 Photosynthetic Apparatus 10
3.2 Oxygen Productivity and Concentration 10

4 Acoustic Variations due to Photosynthesis 12
4.1 Energy and Time Spread Variations 12
4.2 Non Photosynthesis Related Causes of Variation 15
4.3 Effect of Rapid Gaseous Transport on Leaf Blade 16

5 Waveguiding in Posidonia Bubble Layer 18

6 Conclusion 23

References 24

1

Introduction

Prairies of *Posidonia oceanica* Delile represent the most important complex of marine phanerogams in the Mediterranean sea covering an estimated surface area of 20,000 square miles [1]. The development of efficient methods to assess the state of health of the prairies is of considerable interest as standard methods require costly equipment and considerable time.

Acoustic inversion techniques have been proved to be effective and reliable in determining, range integral, physical properties of the upper sediments in shallow water [2]. Recently, research efforts have been directed at using cost-effective, expandable systems consisting of a single sound source and hydrophone [3].

In this paper, the inverse acoustical determination of oxygen productivity of a prairie of *Posidonia oceanica* seagrasses is examined. It was hypothesized and verified experimentally that bubbles of photosynthetic oxygen formed on the leaf blades effected guided wave propagation.

2

Yellow Shark Posidonia Experiments

As part of geo-acoustic inversion experiments (Yellow Shark) in the Giglio basin, off the west coast of Italy, propagation measurements were performed in February and May 1995 over a dense and extensive prairie of *Posidonia oceanica* seagrasses which surrounds Scoglio d'Africa, a minor island of the Tuscan Archipelago. Fig. 1 shows plant distribution and bathymetry. The prairie is particularly dense and extensive thanks to the prevalently sandy nature of the sea bottom which represents the most suitable substratum for the establishment of the plants, and to the gently sloping topography which allows the "matte" to develop over several kilometers.

2.1 Acoustic Measurements Configuration

A sound source (S) and a receiver (R) were positioned in an homogeneous part of the *Posidonia oceanica* prairie where the bathymetry is nearly constant (25 m). The SR distance was 1541 m. In May 1995, the acoustic moorings were repositioned at the same locations as in February 1995 by means of a differential global positioning system (DGPS).

Figure 2 shows the experimental geometry. The source, which was moored 4 m above the bottom, consisted of two flextensional acoustic projectors covering two frequency bands. The projectors were cable connected to their driving amplifiers on board R/V *Alliance*. The receiver was a bottom-moored 4-element vertical array (VA) with hydrophones at 4 m, 10 m, 16 m and 22 m water depths (6 m spacing). The received acoustic data were radio telemetered to the acquisition system on board the ship.

2.2 Broad-Band Acoustic Transmissions

The signals transmitted to measure the band-limited impulse response of the acoustic channel consisted of 3 s, broad-band, waveforms linearly frequency modulated (LFM) over the frequency bands 0.1–0.9 kHz (LF) and 0.8–1.6 kHz (HF). The transmitted waveforms were measured on a reference hydrophone at a distance of 2.3 m from the acoustic centers).

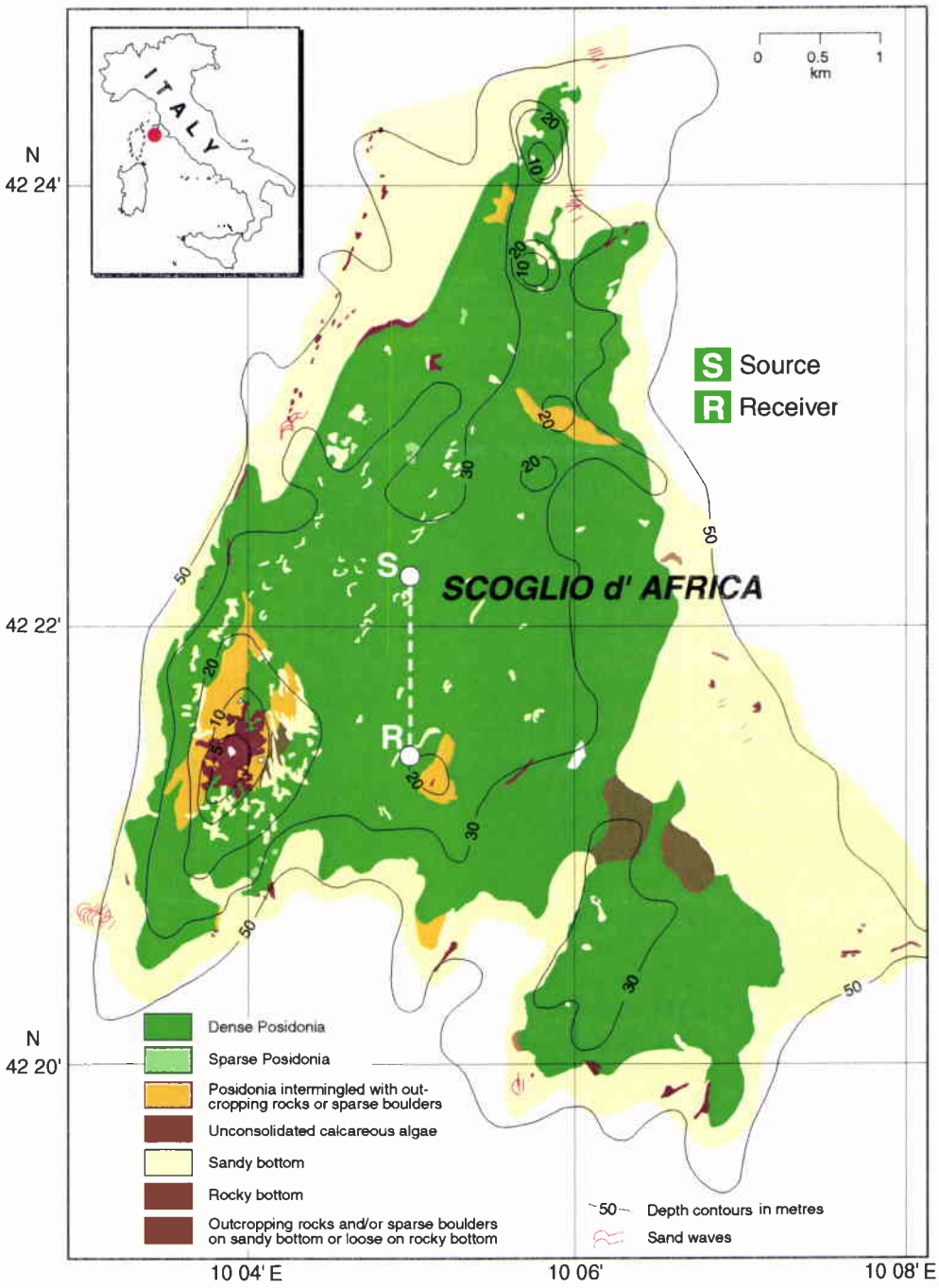

Figure 1 *Map of the Posidonia oceanica prairie at Scoglio d'Africa [after [4]]. The white dots indicate the locations of the bottom-moored sound source (S) and receiving vertical array (R).*

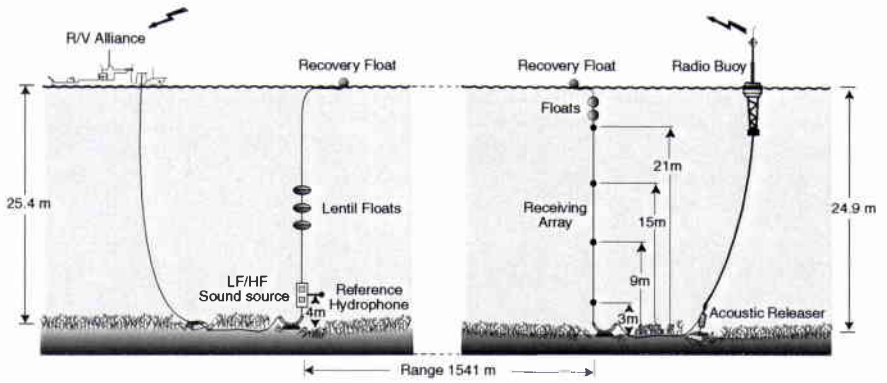

Figure 2 *Experimental geometry showing the positions of the acoustic projectors (left) and hydrophones (left and right).*

The LF and HF bands were transmitted alternatively for variable periods with a pulse repetition rate of 1 min. The transmissions on 3 May 1995 lasted from 1501 to 2308 UTC (afternoon run 99) and on 4 May 1995 from 0404 to 1211 UTC (morning run 100) [5]. The local time (LT) was universal time (UTC) plus 1 hour to exclusion of daylight saving time. The transmitted energies in both bands were maintained at constant levels, verified from the reference hydrophone data. The high-Q flextensionals were not equalized for flat spectrum. The effective bands defined by the frequencies with sound pressure level 3 dB below average, were 329–888 Hz (LF) and 841–1520 Hz (HF) with corresponding time resolutions of 1.8 ms (LF) and 1.5 ms (HF).

2.3 Hydrographic and Irradiance/Oxygen Measurements

CTD, XCTD and XBT profiles were obtained at intervals (< 1 h) at point S. Fig. 3 shows selected sound speed profiles calculated from CTD.

Fig. 4 shows the solar radiation, air temperature, and water temperature from a keel-mounted sensor (4 m depth) during the runs. The light irradiance on the seagrasses decreases with depth and depends on water transparency.

Contemporaneous oxygen and CTD profiles were obtained at point S in February, May, June and July 1997 to support the present study [6]. The environmental conditions in late February were comparable to those in May 1995. Fig. 5 shows a 24 h time series of oxygen concentration measured at 6 water depths. The concentration is the product of the measured percentage of saturation, corrected for measured temperature and pressure and the calculated solubility for given temperature and salinity.

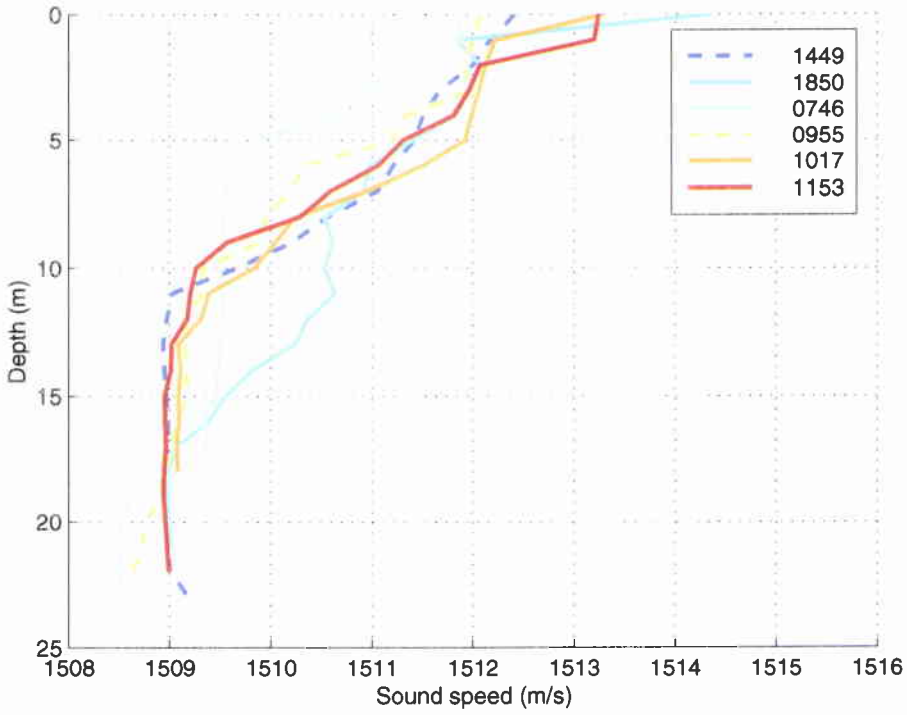

Figure 3 *Sound speed profiles at point S calculated from CTD alone during the acoustic transmissions. Indicated times are UTC. The dashed lines are two reference profiles discussed in the text.*

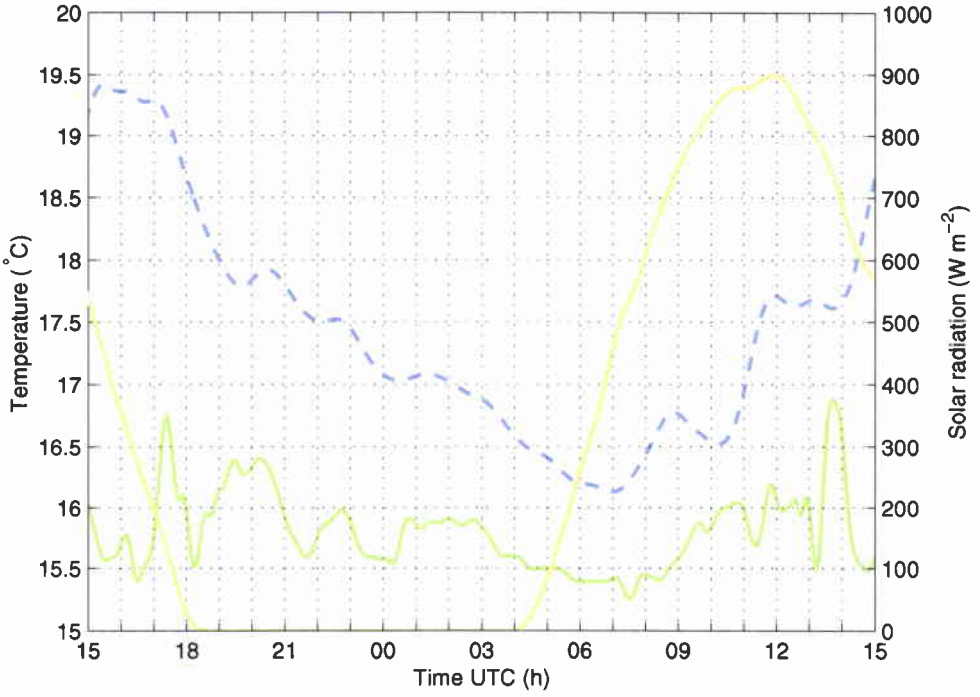

Figure 4 *Air (dashed line) and water (solid line) temperatures (left scale), and solar radiation (right scale) measured at point S during the acoustic transmissions. Sunset and sunrise were at 1816 and 0417 UTC (=LT−1).*

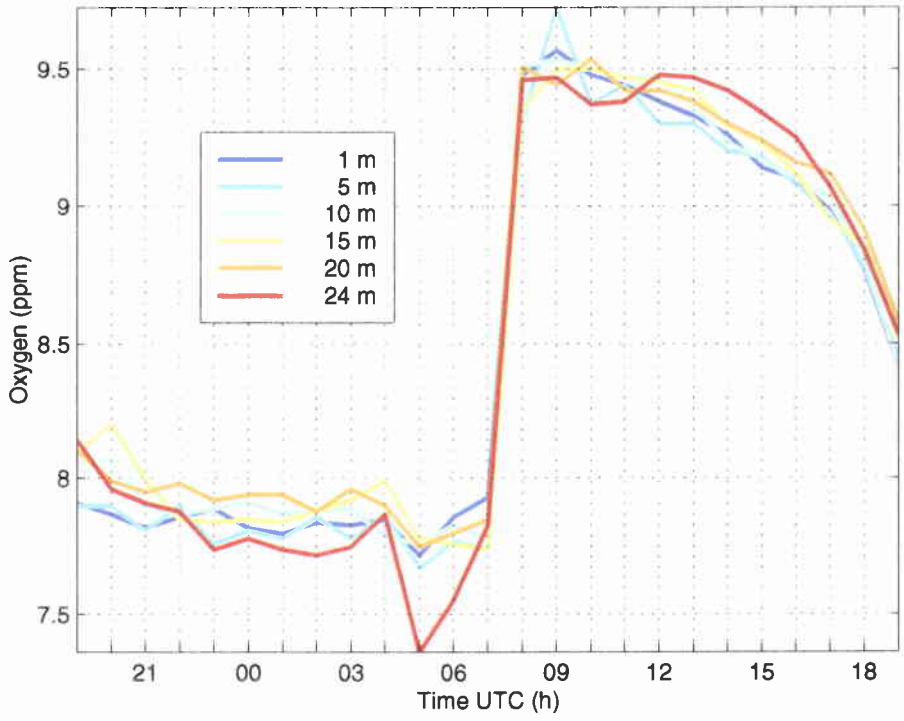

Figure 5 *Oxygen concentration versus time of day at different water depths. The profiles were measured at point S on 24 and 25 February 1997. Sunrise and sunset were at 0606 and 1700 UTC (=LT−1).*

2.4 Posidonia Plants and Substratum

The measured depth profile along the SR transect varied by less than 1 m.

A film record of the prairie and a sample of the plants and matte was obtained for examination. The leaf blade width and thickness are approximately 1 cm and 180 μm [7]. Average number of blades per shoot of 7, blade surface of 73 cm^2 and total blade surface per shoot of 506 cm^2 were determined from a 40×40 cm sample collected at 25 m depth [4]. The shoot density is approximately 10^3 per m^2.

The matte is formed by the intertwining of various strata of rhyzomes, roots and trapped sediments [8]. In the investigated area the sediments are made of medium and coarse sands, primarily organogenous. A detailed analysis of the mass properties was not available. The geo-acoustic properties of the matte are poorly known. *In situ* measurements would be necessary to obtain reliable values of sound speed and attenuation. The sound speed was expected to be low ($c < 1650$ m s^{-1}) due to the uneven nature of the water saturated sands with low permeability, the presence of slow materials (rhyzomes and roots) and gas from the decomposition of organic material. Attenuation was high (> 1 dB/λ) as acoustic energy of a boomer hardly penetrated the matte layer due to absorption and scattering. Comparable conditions are encountered with soft porous sediments with high gas content. There is no evidence that oxygen production rate modifies sound speed and attenuation in the matte except for transient mass flows of gas to the rhizomes and roots at dark-to-light transition and the reverse at light-to-dark. The matte thickness and bottom morphology were not well resolved by the boomer.

2.5 Time-Varying Waveguide Impulse Response

The LF and HF signals received on the 4 VA elements were matched-filtered using the transmitted waveforms as reference. This provided band-limited impulse responses of the waveguide at 1 min intervals. Fig. 6 shows two consecutive LF snapshots taken early morning. Although transmitted energy spectra were not flat, especially in the LF band, the responses were suitable for our purposes.

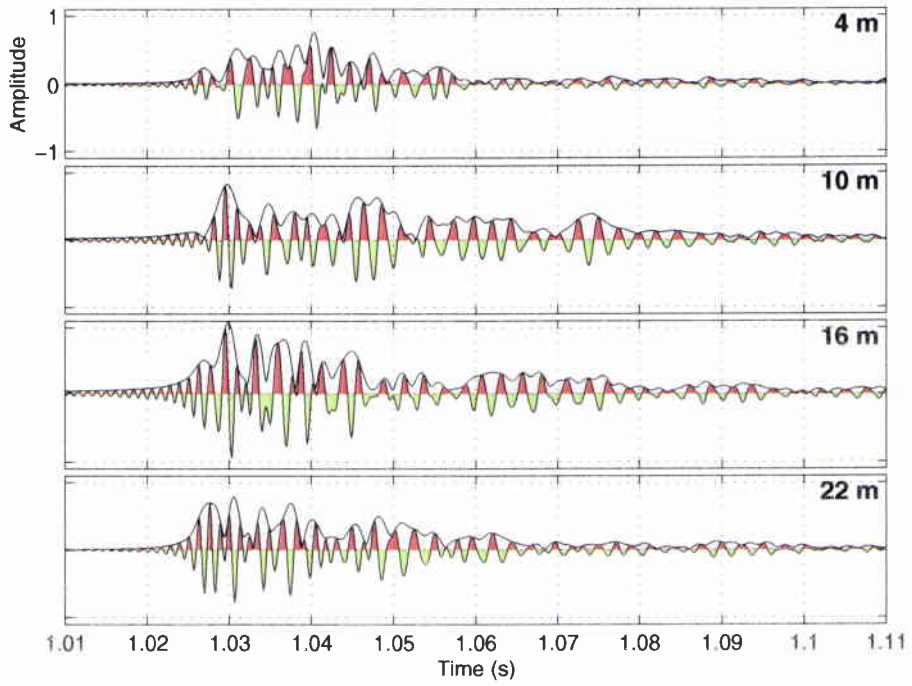

(a) 0728 UTC

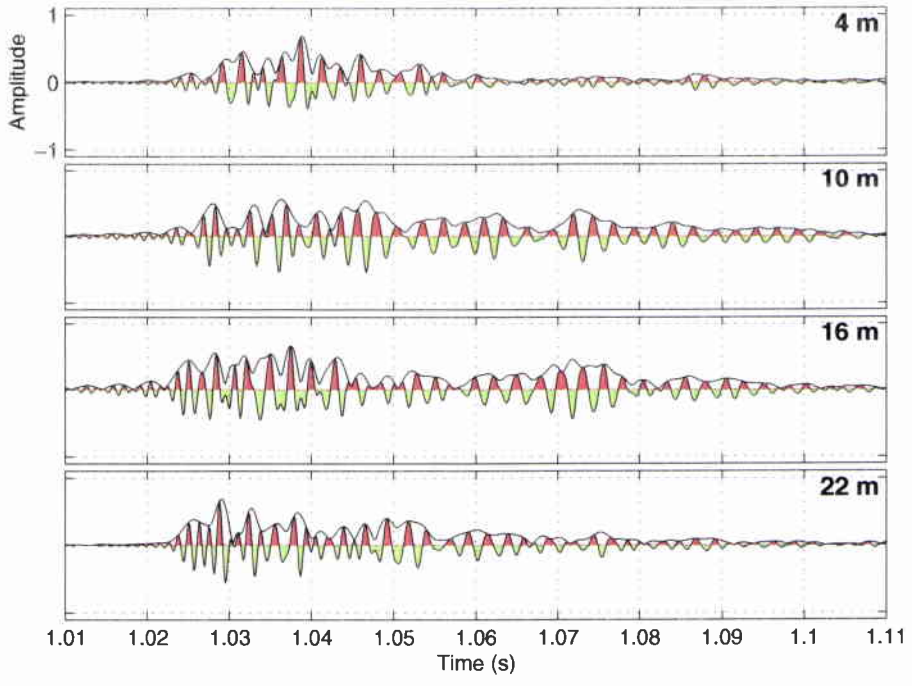

(b) 0729 UTC

Figure 6 *Snapshots of the LF-band impulse response of SR waveguide measured on the 4 VA elements. Water depths are indicated.*

3

Oxygen Measurements in Posidonia Waters

In coastal waters, oxygen content is determined by air-sea flux and specific environmental and biomass conditions including photosynthesis of marine plants, life processes of animals, and decomposition of organic materials.

3.1 Photosynthetic Apparatus

Seagrass leaf morphology allows for maximum release of photosynthetic oxygen to the ambient medium.

Posidonia oceanica (L.) Delile is an endemic phanerogam of the Mediterranean sea. Its long ribbon-shaped leaves are grouped in shoots which develop on various substrates in 1–40 m water depths.

The *P. oceanica* leaf blade consists of a monolayered epidermis and a 3–4 layered mesophyll [7]. The major site of photosynthesis is the epidermis where chloroplasts are densely arranged in small radially elongated cells. The outer wall of epidermidal cells is formed by an outer continuous layer (cuticle) and an underlying thick porous region with irregularly shaped cavities. The lacunar system is constituted by connected air channels within the mesophyll. The particularly small dimensions of the lacunar system is a distinctive feature of *P. oceanica*.

The major driving force for exchange of gases between seawater, epidermal cells and lacunar system is photosynthesis. Respiratory activity is nearly an order of magnitude lower and largely involves the lacunar system. Unlike other aquatic plants, gaseous exchanges with seawater are effected by molecular diffusion as there are no stomata. The processes of oxygen uptake for respiration and release of photosynthetic oxygen are constrained by the diffusion boundary (unstirred) layer, and to a lesser extent, by the cuticle and cell wall.

3.2 Oxygen Productivity and Concentration

Photosynthesis by *P. oceanica* substantially increases the quantity of oxygen in dissolved and bubble form. A productivity of 5–10 g of fixed carbon per m^2 per

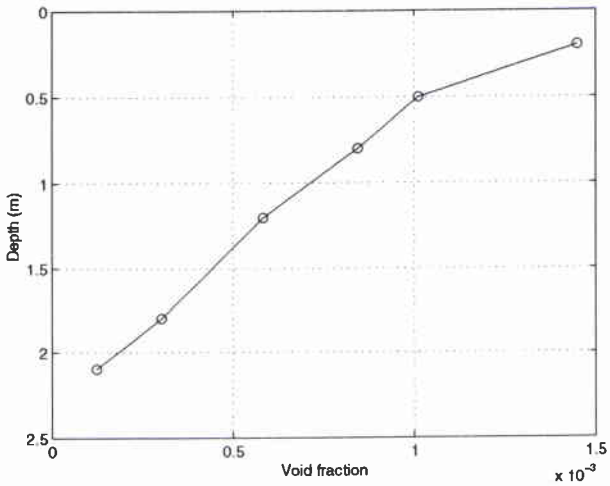

Figure 7 *Oxygen void fraction profile below the sea surface calculated from measurements at point S at 1100 UTC on 25 February 1997.*

day is reported [9], and according to some authors it can attain 20 g m^{-2} day^{-1}. Based on these data it was calculated that at least 3 l of oxygen per m^2 per day is produced by plants at 25 m water depth and 15 °C. Values up to 14 l m^{-2} day^{-1} have been reported [4].

The 1997 survey at Scoglio d'Africa showed that the time variation of oxygen concentration in *P. oceanica* waters was determined principally by the daily cycle of oxygen productivity. Comparison of different months showed circadian productivity variations. In Fig. 5, a rapid increase of concentration, 1 h after sunrise, follows the start of photosynthesis. After reaching a peak value of 9.5 ppm, 2 h after sunrise, concentration gradually decreases until dawn. The time of occurence and rate of change of these variations were in agreement with irradiance-productivity measurements on the plants obtained under similar conditions [9]. Due to the nearly isothermal (14.2–14.7 °C) conditions the concentration was constant with depth (±0.1 ppm) except immediately above the plants (24 m) where it appeared to be directly influenced by respiratory activity of flora and fauna (the valleys and peaks). As discussed below, the time variations of oxygen concentration in the water column were closely related to the gas void fraction (volume of gas in bubble form per volume of water) within the *Posidonia* leaf layer.

From CTD and oxygen data, it was calculated that in February, oversaturation (undissolved oxygen) conditions occurred 2 h after sunrise in a 2 m layer below the sea surface. In June, these conditions persisted overnight due to higher temperature and photosynthetic activity [6]. Fig. 7 shows the estimated oxygen void fraction *versus* depth in February.

4

Acoustic Variations due to Photosynthesis

It is demonstrated that an abrupt and marked change of the waveguide propagation characteristics from dark to light can be attributed to photosynthetic oxygen bubbles generated by *P. oceanica.*

4.1 Energy and Time Spread Variations

The total time dispersion of the LF and HF impulse responses of the waveguide were, at all time, greater than 120 ms (Fig. 6) and 40 ms. In the HF band, the late arrivals were strongly attenuated. The ever present air bubbles near the surface and seagrass lacunar gas contributed to the time dispersion.

To demonstrate the oxygen effect, the time-varying waveguide responses $g(t)$ were first defined by their total energy and time spread. By considering $|g(t)|^2$ as an energy density in time, energy time spreading was characterized by the standard deviation

$$\sigma_t^2 = \langle t^2 \rangle - \langle t \rangle^2 \tag{1}$$

where the mean time $\langle t \rangle$ is defined as

$$\langle t \rangle = \int t|g(t)|^2 dt \tag{2}$$

and $\langle t^2 \rangle$ is defined similarly.

Figures 8 and 9 show the variations of total energy and time spread for the two frequency bands. The dots correspond to the 1 min repeated measurements. The lines represent 1 h averages calculated by cubic spline smoothing, except for the sparse afternoon HF measurements. For each frequency band, energies were normalized to their maximum.

For HF, received energy was systematically less near the surface (4 m) and bottom (22 m). For LF, only surface energy was lesser.

The high degree of correlation between the energy and time spread variations is consistent with the concomitant effects of scattering, absorption and dispersion expected from a medium with time- and depth-dependent bubble population.

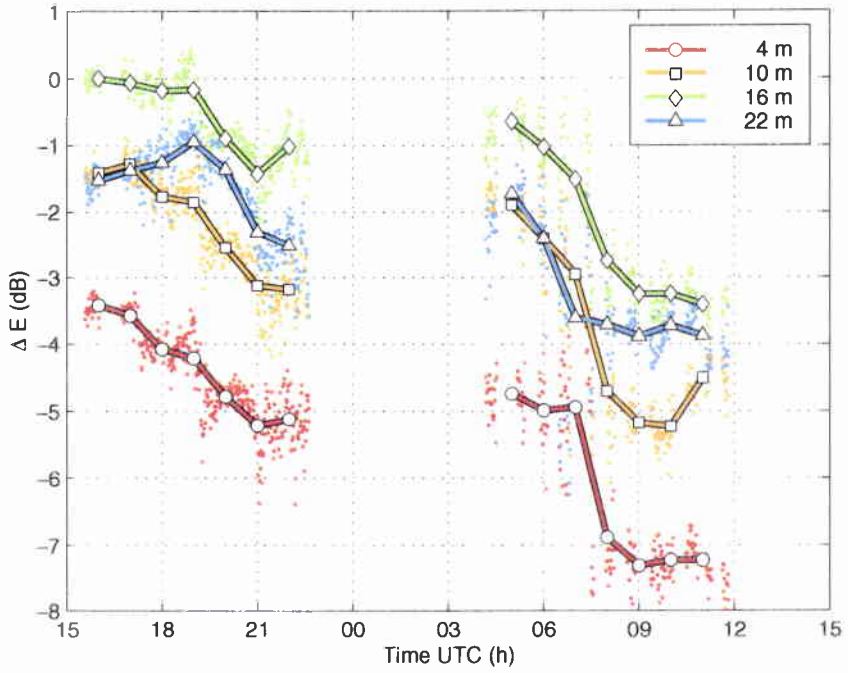

(a) Energy, LF

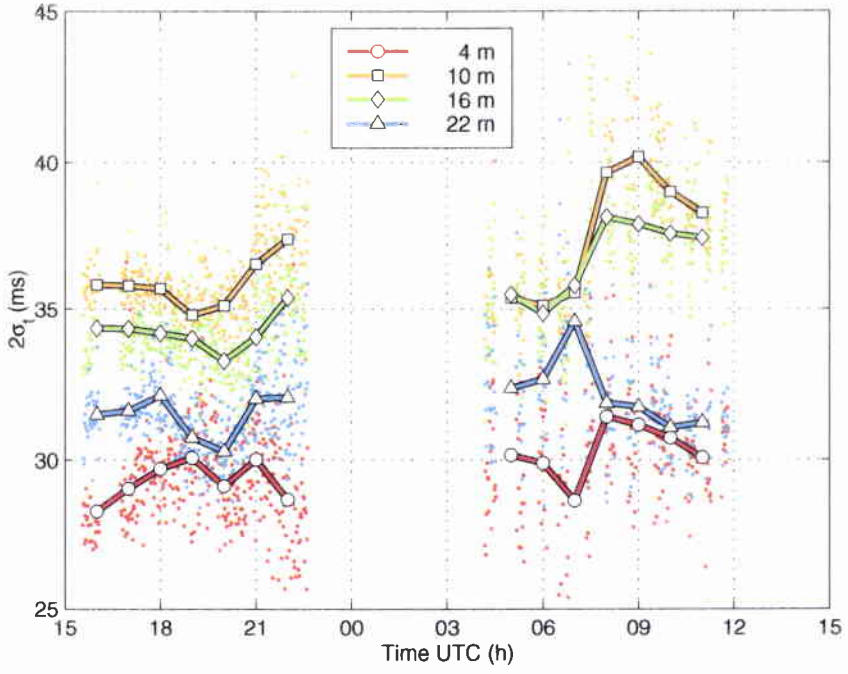

(b) Time spread, LF

Figure 8 *Energy and time spread of the waveguide impulse response in the frequency band 0.1–0.9 kHz (LF).*

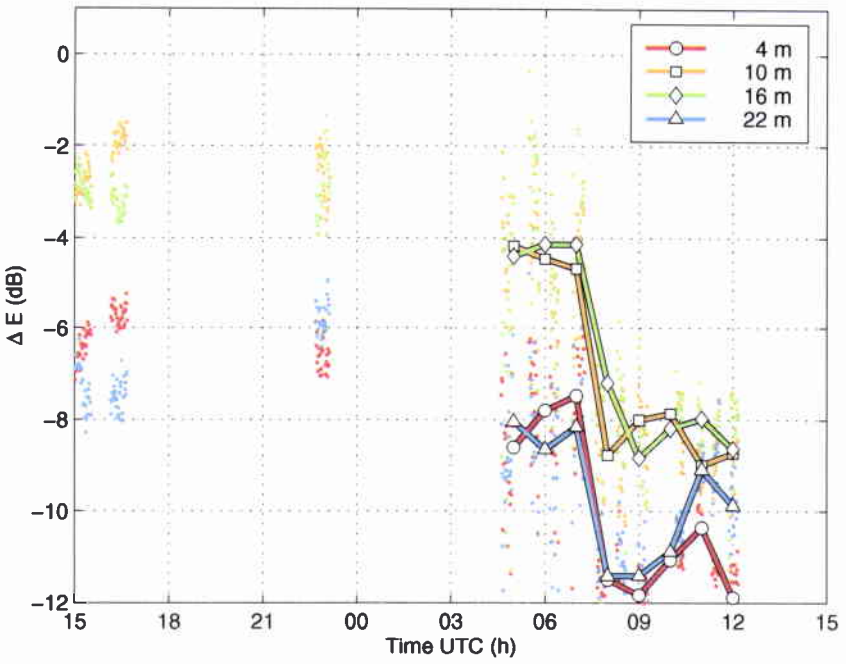

(a) Energy, HF

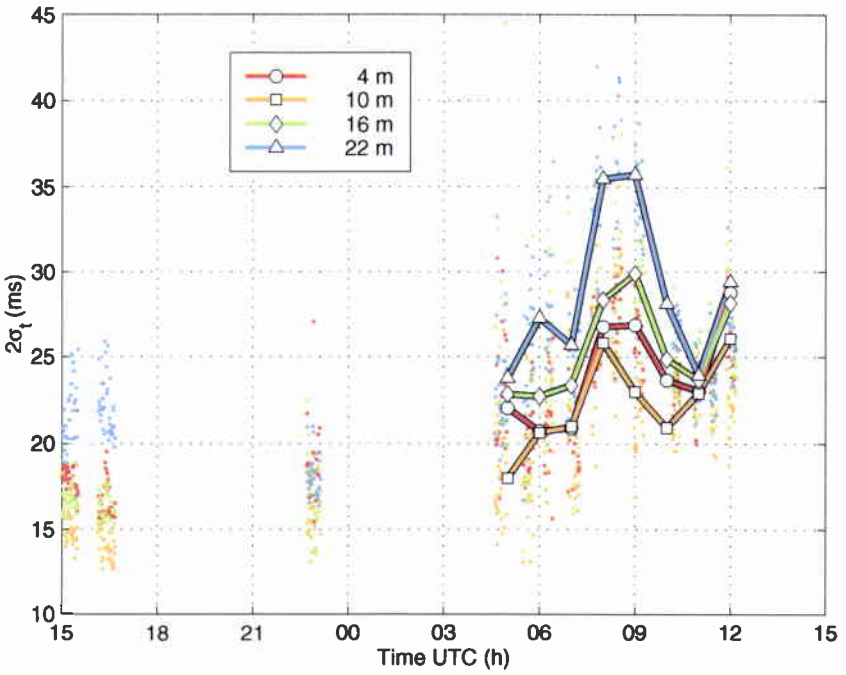

(b) Time spread, HF

Figure 9 *Energy and time spread of the waveguide impulse response in the frequency band 0.8–1.6 kHz (HF).*

In both LF and HF bands, received energies decreased dramatically when active photosynthesis started. The excess attenuations are depth dependent and greater for HF (3–5 dB) than for LF (2–3 dB). The rate of decrease is higher for HF than for LF.

For LF, step increases (3–5 ms) of time spread occurred at depths of 10 m and 16 m. For HF, transient increases (5–10 ms) occurred with the highest peak above the leaf layer (22 m). It is conjectured that there is a causal relationship between the increased oxygen productivity rate and these peaks.

The 1 min spaced measurements showed a very sharp transition in the arrival structure between 0728 UTC and 0729 UTC (Fig. 6) explained below.

The acoustic variation corresponds with increased oxygen concentration followed by a gradual decay (Fig. 5), taking into account the solar time difference between May and February measurements.

4.2 Non Photosynthesis Related Causes of Variation

The main variations were not due to thermal variability. This is proved unequivocally by the fact that the largest differences of energy and time spread between mid afternoon and morning corresponded to nearly identical CTD-derived sound speed profiles (3 May 1449 UTC and 4 May 0955 UTC, dashed lines in Fig. 3). All profiles (only a few are displayed in Fig. 3) showed variability in sound speed gradient (max. $\Delta c = 3$ m s^{-1} at 10 m depth) with no profound effect upon propagation. Range dependence of sound speed profile was negligible because of the short length and central location of the SR transect (Fig. 1).

Because of calm sea and low (1–6 m s^{-1}) wind speed conditions, production of air bubbles due to wave action was trivial in comparison to photosynthetic oxygen. There was no correlation between the dominant acoustic variation and wind speed.

The diversity and abundance of fish in *P. oceanica* seagrass beds are known to increase at night due to immigration of reef fish and movement of diurnal planktivores from the water column to sheltering sites beneath the foliage. These movements could explain the greater scatter of the measurements in the evening and early morning (dots in Figs. 8 and 9). For LF, there were well defined time periods for which attenuation was greater than the trend (e.g. at total dark roughly 1 h after sunset).

4.3 Effect of Rapid Gaseous Transport on Leaf Blade

The particularly rapid change of acoustic propagation features 3 h after sunrise (500 W m^2 solar radiation) were explained by a sudden increase of oxygen void fraction within the seagrass layer. The mechanisms described were adapted from a general account on gaseous movement in seagrasses which does not deal specifically with *P. oceanica* species [10].

From measured average leaf blade dimensions and density, the leaf-volume fraction is approximately 6 10^{-3}. It was estimated that the volume fraction of porous region beneath the cuticle does not exceed 3 10^{-5}. The fraction of lacunar air spaces is much smaller.

As photosynthetic tissue is concentrated in the epidermidis, the epidermal cells experience a rapid build-up of oxygen at dark-to-light transition. The resulting diffusion gradient causes oxygen to diffuse towards the ambient medium and the lacunar system, in proportions which depend on the diffusion resistance of the outward and inward pathways, size of the leaf and physical characteristics of seawater and lacunar gases. Under *in vivo* pressurized conditions (3.5 10^5 Pa at 25 m water depth) the unstirred layer, cuticle and cell-wall provide large resistance to diffusion.

Initially, at low irradiance, oxygen accumulates in the porous wall beneath the cuticle and in the small air spaces of the mesophyll. This causes an increase of oxygen concentration and pressure within the leaf blade. Even under rapid stirring conditions, pressures greater than 2 10^4 Pa have been measured in comparable seagrasses. A continuous stream of bubbles is produced from any cut surface of leaves, rhyzomes or roots. The initial pressurization causes a transient mass flow of lacunar gas to the rhizomes and roots.

Then, with increasing irradiance, oxygen starts to diffuse into seawater and form bubbles which adhere to the leaf blade. Acoustic measurements indicated that the phenomena occurred in a matter of seconds (Fig. 6). Though free large gas bubbles in water tend to collapse by gas diffusion forced by surface tension or rise rapidly to the surface by buoyant action, the continuous oxygen supply and wall-adhesion effect maintain a large void fraction of oxygen bubbles near the sea bottom in addition to oxygen in the porous wall and gas in the lacunar system. At light, bubbles of visible size on the leaf blades and rising to the surface are commonly observed by divers.

During steady-state photosynthesis, an equilibrium is established between oxygen production rate and processes of bubble formation and dissolution in seawater which mostly depend on the degree of stirring. The photosynthetic oxygen progressively enriches the water column (Fig. 5) and contributes to oxygen supersaturation in the surface layer.

The sequence of events described is consistent with the fact that, after sunrise, LF energy decreased earlier at the bottom (triangle) than at the surface (circle) [Fig. 8(a)]. It is also noted that, during the preceding afternoon, bottom energy variation differed to that of the water column.

The above analysis established a causal relationship between photosynthesis daily cycle and measured acoustic variations.

5

Waveguiding in Posidonia Bubble Layer

The cutoff frequencies of the SR waveguide for modes 1, 10 and 18 are respectively 45 Hz, 862 Hz and 1589 Hz for $c = 1600$ m s^{-1}.

Simulation results indicated that Pekeris models with *in situ* water sound speed profiles $c(z)$ and half-space bottom sound speeds in a plausible range c =1550–1650 m s^{-1} were not suitable to the general character of the waveguide response. The most noticeable differences were, for the measurements, the greater attenuation of low-order modes and higher degree of intra-modal dispersion.

A consequence of time- and depth- dependent bubble populations was that the actual sound speed profiles in water were different to those calculated from temperature, salinity and depth alone (Fig. 3).

The responses were modeled by introducing, over the bottom (b) and below the surface, layers (p, s) with sound speed smaller than the water (w) medium ($c <$ 1509 m s^{-1}) [Fig. 10]. The p-layer thickness was taken as the average height ($\Delta z_{\rm p} =$ 0.75 m) of the plants and the s-layer thickness as the limit water depth ($\Delta z_{\rm s} =$ 2 m) of supersaturation conditions. The speeds were varied in the range $c_{\rm p}$ =500–1500 m s^{-1}. Densities $\rho_{\rm s}$ and $\rho_{\rm p}$ were taken as equal to $\rho_{\rm w} = 1.03$ g cm^{-3} as small ($U < 10^{-3}$) bubble void fractions have a negligible effect upon density compared to compressibility.

The acoustic properties of the lower and upper layers determined how the propagated broad-band energy interacted with the boundaries. They acted as additional waveguides, parallel to the main one, where modes could propagate depending on order and frequency [11].

Fig. 11 shows calculated low-frequency asymptotic sound speed and corresponding transition frequency of the first two modes *versus* gas void fraction in the *Posidonia* leaf layer. The sound speed was calculated from the Wood's equation (simple mixture theory) [12],

$$c_{\rm p} = (E_{\rm g}E_{\rm w})^{1/2} / [U\rho_{\rm g} + (1-U)\rho_{\rm w}]^{1/2}[UE_{\rm g} + (1-U)E_{\rm w}]^{1/2} \quad (3)$$

where $E_{\rm g} = \gamma p_{\rm A}$ and $E_{\rm w} = \rho_{\rm w} c_{\rm w}^2$ are the bulk moduli of elasticity of gas and water,

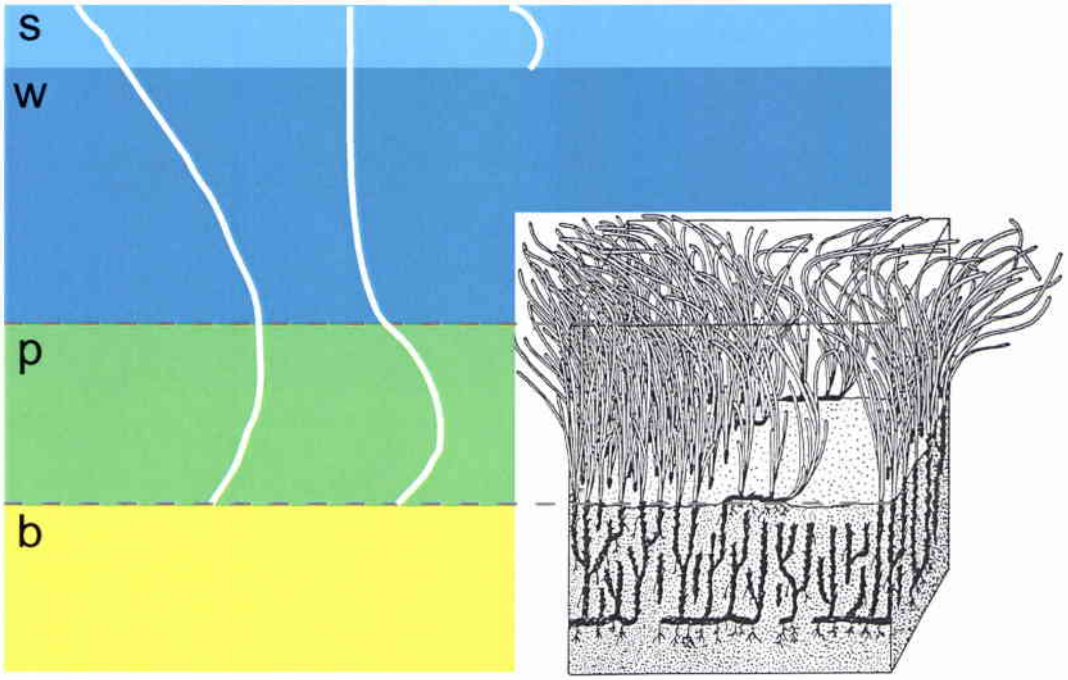

Figure 10 *Posidonia bubble waveguides: (s) surface, (w) water, (p) Posidonia, (b) matte bottom. The white curves show the evolution of mode 1 shape from night (left) to day (right)*

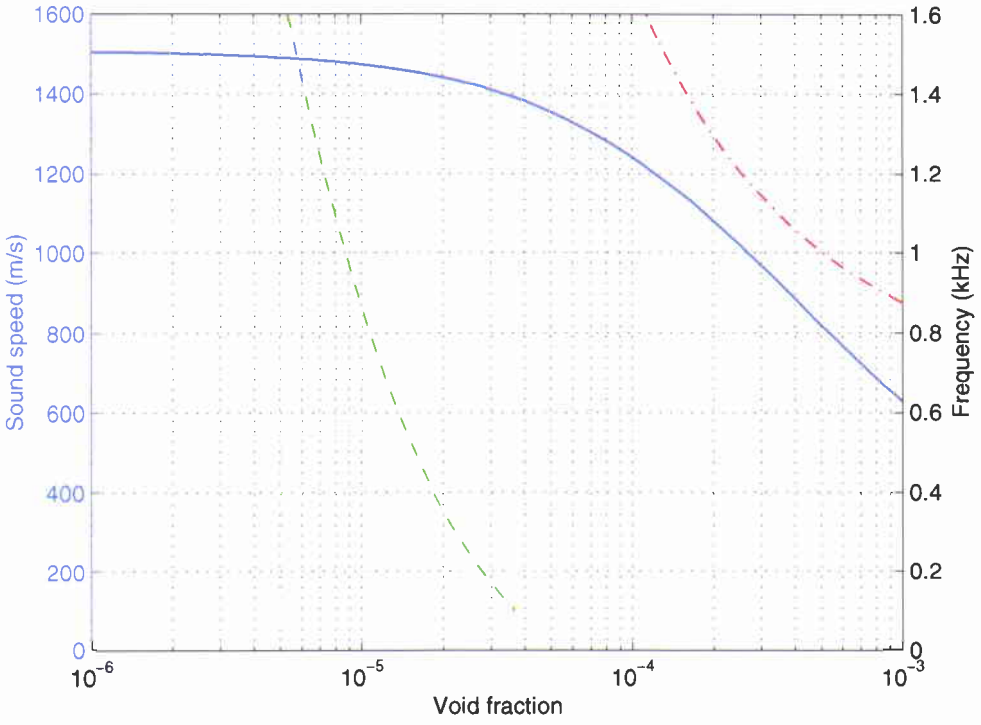

Figure 11 *Low-frequency asymptotic sound speed (solid line) and transition frequency of modes 1 (dashed line) and 2 (dash-dotted line) versus oxygen plus gas void fraction of bubbles in a Posidonia leaf layer.*

$\gamma = 1.4$ is the ratio of specific heats of gas (air or oxygen), $\rho_g = 1.43$ g l^{-1} (oxygen) and p_A is the ambient pressure.

The mth mode transition frequency f_m is given by [11]

$$\begin{aligned} f_m &= c_p/\lambda_m \\ \lambda_m &= 4\pi\Delta z_p \sin\phi/ \\ &\quad (2m-1)\pi - 2(\rho_b/\rho_p)\phi/\sin\theta \\ \phi &= \arccos(c_p/c_w) \\ \theta &= \arccos(c_p/c_b) \end{aligned} \tag{4}$$

For the matte bottom, density $\rho_b = 1.8$ g cm^{-3} and sound speed $c_b = 1600$ m s^{-1} were assumed.

For the HF transmissions, gas void fractions in the range 5 10^{-6}–10^{-5} were sufficient for mode 1 propagation in the seagrass layer. For fractions increasing from 10^{-4} the frequency components of mode 2 were gradually trapped. For LF, mode 1 began to travel in the seagrass layer for fractions greater than 10^{-5}. For rapid increase to values greater than 4 10^{-5} mode 1 dissapeared suddenly from the water layer. Mode 2 traveled in the water layer for all low frequencies. The transition frequency curves in Fig. 11 shift toward the left-bottom corner for increasing thickness of the seagrass layer and right side for increasing sound speed in the matte layer.

Comparison of waveguide responses between dark and light confirmed the predicted mode filtering effect. Before the initial discharge of oxygen from the plants [Fig. 6(a)] faster mode 1 arrivals are resolved with large amplitude by comparison to slower high-order mode arrivals. The downward shift of the mode shape increasing with frequency is apparent. After discharge [Fig. 6(b)], the amplitude of mode 1 arrivals had decreased substantially in the water layer as being trapped in the seagrass layer. The trapped and higher order modes were attenuated as a result of increased scattering and absorption in the bubble medium.

Fig. 12 shows the normalized time-frequency energy distribution of two consecutive waveguide responses measured at 16 m depth (Fig. 6). For mode 1, the decreased high-frequency energy content and increased low-frequency time dispersion after oxygen discharge (0729 UTC) are apparent. There is a marked change of curvature in the group delay *versus* frequency characteristics of the first two modes. The dispersion is primarily due to geometry and sound speed gradients of the multilayered waveguide but also to intrinsic dispersion which takes place within the bubble medium.

Waveguiding in the near-surface layer [13] occurred later in the day when the gas void fraction increased. The effect was less marked because of pressure-release upper boundary, the gradual decrease of void fraction with depth (Fig. 5) and the downward refracting sound speed gradient (Fig. 7).

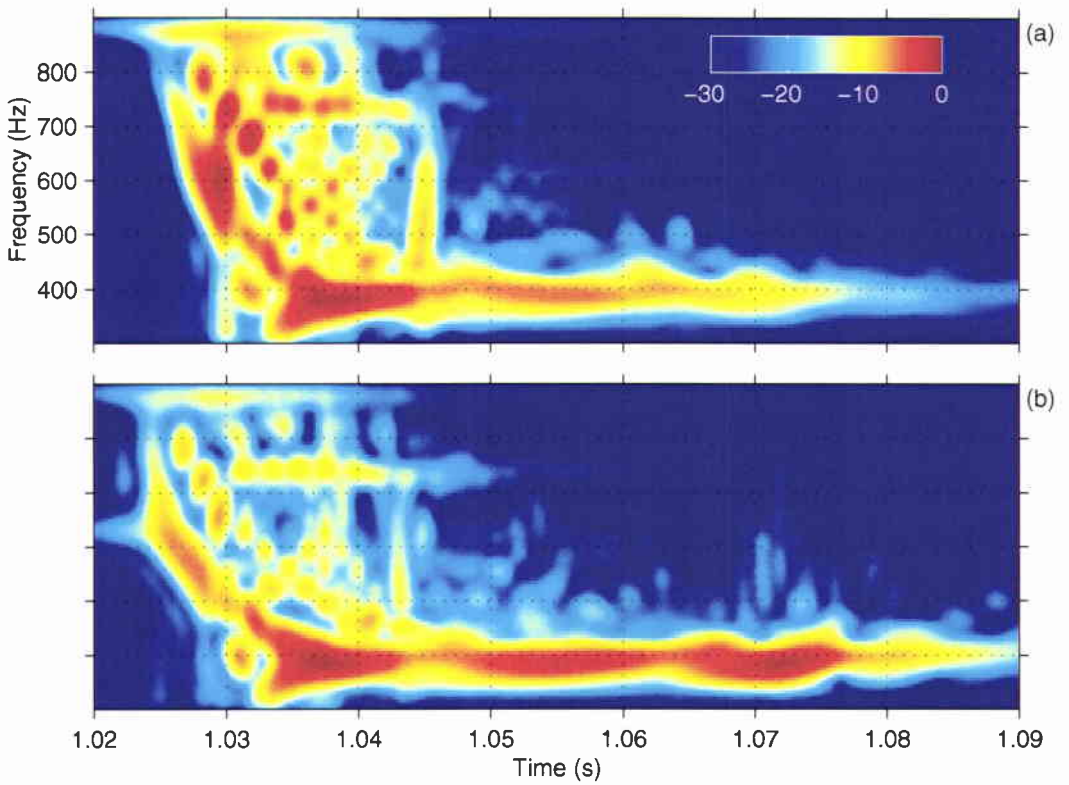

Figure 12 *Change of frequency-dependent attenuation and time dispersion characteristics of the main waveguide in less than 1 min: (a) 0728 UTC, (b) 0729 UTC LF receptions at 16 m water depth.*

6

Conclusion

Experimental results proved unequivocally that significant variations of acoustic waveguide propagation characteristics—attenuation and time dispersion—were due to bubbles of photosynthetic oxygen produced by the *P. oceanica* seagrasses.

The acoustic variations were explained by time-dependent waveguiding in the seagrass oxygen-bubble layer, and to a lesser extent, in the near-surface gas-bubble layer.

Modeling results indicated that the inverse problem of determining gas and oxygen void fractions in the seagrass layer could be solved. Parameters such as surface density and photosynthetic efficiency of *P. oceanica* can be derived from the variations of inverted void fractions.

These results may be applicable to the monitoring of *P. oceanica* and other seagrasses in the Mediterranean and other oceans.

References

[1] Cinelli, F., Fresi, E., Lorenzi, C., and Mucedola, A., editors (1995) *La Posidonia oceanica.* Rivista Marittima.

[2] Wilson, J.H., Rajan, S.D. and Null, J.M., editors (1996) *IEEE Journal of Oceanic Engineering,* special issue on Inversion Techniques and the Variability of Sound Propagation in Shallow Water **21**, 4.

[3] Hermand, J.-P. (1999) Broad-band geoacoustic inversion in shallow water from impulse response measurements on a single hydrophone: Theory and experimental results, *IEEE Journal of Oceanic Engineering,* **21**, 4, pp. 41–66.

[4] Cinelli, F. (1992) *Mappatura delle Praterie di Posidonia oceanica (L.) Delile intorno alle Isole Minore dell'Arcipelago Toscano,* Ministero della Marina Mercantile, Ispettorato Centrale per la Difesa del Mare.

[5] Hermand, J.-P., Spina, F., Nardini, P. and Baglioni, E. (1996) *Yellow Shark broad-band inversion experiment: Environmental data 1994–1995,* SACLANTCEN CD-ROM Yellow Shark series YS-2, SACLANT Undersea Research Centre, La Spezia, Italy.

[6] Nascetti, P. (1998) *Rilievi stagionali e circadiani della produzione di ossigeno di praterie di Posidonia oceanica in supporto ad uno studio di inversione acustica,* Tesi di Laurea in Scienze Biologiche, Facoltà di Scienze Fisiche, Matematiche e Naturali.

[7] Colombo, P. M., Rascio, N. and Cinelli, F. (1983) *Posidonia oceanica* (L.) Delile: A structural study of the photosynthetic apparatus, *Marine Ecology* **4**, 2, pp. 133–145.

[8] Colantoni, P. (1995) Sediments of the Posidonia oceanica meadows. pp. 48–55. In [1].

[9] Libes, M. (1986) Productivity-irradiance relationship of Posidonia oceanica and its epiphytes, *Aquatic Botany* **26**, pp. 285–306. Elsevier Science Publishers B. V., Amsterdam.

[10] Larkum, A.W.D., McComb, A.J. and Shepherd, S.A. (1989) *Biology of Seagrasses.* Elsevier, New York.

[11] Hermand, J.-P. and Soukup, R. (1996) Broadband inversion experiment Yellow Shark 95: Modelling the transfer function of a shallow-water environment with

a range-dependent soft clay bottom. In Papadakis, J. S., editor, *Proceedings of the Third European Conference on Underwater Acoustics,* pp. 931–936, Heraklion, Crete.

[12] Medwin, H. and Clay, C.S. (1998) *Fundamentals of Acoustical Oceanography.* Academic Press, New York.

[13] Farmer, D.M. and Vagle, S. (1989) Waveguide propagation of ambient sound in the ocean-surface bubble layer, *Journal of the Acoustical Society of America* **86**, 5, pp. 1897–1908.

Document Data Sheet

Security Classification		Project No.
UNCLASSIFIED		01-B
Document Serial No.	**Date of Issue**	**Total Pages**
SM-366	December 1999	31 pp.

Author(s)

Hermand, J.-P., Nascetti, P., Cinelli, F.

Title

Inverse acoustical determination of photosynthetic oxygen productivity of posidonia seagrass.

Abstract

As part of geoacoustic inversion experiments (Yellow Shark) in the Giglio basin, off the west coast of Italy, low frequency, broad-band propagation measurements were performed in the winter and spring of 1995 over a dense and extensive prairie of Posidonia seagrasses which surrounds Scoglio d'Africa, a minor island of the Tuscan Archipelago. The purpose of the measurements was to determine the applicability of model-based, geoacoustic inversion techniques developed for marine sediments to the monitoring of oxygen synthesis by Posidonia.

A dual-flextensional acoustic projector and a 4-element vertical receiving array were positioned at 1541 m distance in an isobath (25 m water depth), dense and homogeneous part of the Posidonia prairie. The waveguide impulse response was measured during one day by 1 min repeated and alternated transmissions of 3 s chirp signals with frequency bands 0.1-0.9 kHz and 0.8-1.6 kHz.

The water sound speed profiles calculated from repeated CTD measurements were slightly downward refracting and exhibited little temporal variability except for mild surface heating in the afternoon. Contemporaneous oxygen and CTD profiles as a function of daytime and season were obtained in 1997 to support the present study.

In this paper acoustic, solar radiation, oxygen and CTD data are analyzed and discussed. The analysis shows strong correlation between photosynthesis and the impulse response of the acoustic waveguide. The most evident feature is an abrupt and marked change of attenuation and time dispersion characteristics at the onset of photosynthesis. Frequency- and depth-dependent rapid variations of received energy (2-5 dB) and time spread (3-10 ms) are observed. The time of occurrence and rate of change of these variations are consistent with solar time and oxygen concentration measured *in situ*. The phenomena is attributed to bubbles of photosynthetic oxygen formed on the Posidonia leaf blades. The bubble layer creates an absorbing, dispersive, low-speed, thin parallel waveguide which modifies interaction of acoustic energy with the Posidonia "matte". It is demonstrated that, after sunrise, low-order modes begin to travel in the seagrass layer, absorbing a portion of acoustic energy from the main waveguide. A similar effect can occur in a near-surface waveguide when supersaturation (undissolved oxygen) conditions obtain.

Modeling results indicate that the inverse problem of determining gas and oxygen void fractions in the seagrass layer could be solved. Parameters such as surface density and photosynthetic efficiency of Posidonia can be derived from the variations of inverted void fractions.

These results may be applicable to the monitoring of the state of health of Posidonia and other seagrasses in the Mediterranean and other oceans.

Issuing Organization

North Atlantic Treaty Organization
SACLANT Undersea Research Centre
Viale San Bartolomeo 400, 19138 La Spezia, Italy

[From N. America: SACLANTCEN (New York) APO AE 09613]

Tel: +39 0187 527 361
Fax:+39 0187 527 700

E-mail: library@saclantc.nato.int

The SACLANT Undersea Research Centre provides the Supreme Allied Commander Atlantic (SACLANT) with scientific and technical assistance under the terms of its NATO charter, which entered into force on 1 February 1963. Without prejudice to this main task - and under the policy direction of SACLANT - the Centre also renders scientific and technical assistance to the individual NATO nations.

SACLANT Undersea Research Centre
Viale San Bartolomeo 400
19138 San Bartolomeo (SP), Italy

tel: +39 0187 527 (1) or extension
fax: +39 0187 527 700

e-mail: library@saclantc.nato.int

NORTH ATLANTIC TREATY ORGANIZATION